

Density Functional Theory Studies of Oxygen Affinity of Small Au Nanoparticles

Hyunwoo Ha¹, Kihyun Shin² and Hyun You Kim^{1†}

¹Department of Materials Science and Engineering, Chungnam National University,
Daejeon 34134, Republic of Korea

²Department of Materials Science and Engineering, KAIST, Daejeon 34141, Republic of Korea

(Received December 12, 2016 : Revised December 12, 2016 : Accepted February 17, 2017)

Abstract Through density functional theory calculations, to provide insight into the origins of the catalytic activity of Au nanoparticles (NPs) toward oxidation reactions, we have scrutinized the oxygen adsorption chemistry of 9 types of small unsupported Au NPs of around 1 nm in size (Au13, Au19, Au20, Au25, Au38, and Au55) looking at several factors (size, shape, and coordination number). We found that these NPs, except for the icosahedral Au13, do not strongly bind to O₂ molecules. Energetically most feasible O₂ adsorption that potentially provides high CO oxidation activity is observed in the icosahedral Au13, our smallest Au NP. In spite of the chemical inertness of bulk Au, the structural fluxionality of such very small Au NP enables strong O₂ adsorption. Our results can support recent experimental findings that the exceptional catalytic activity of Au NPs comes from very small Au species consisting of around 10 atoms each.

Key words density functional theory, gold, heterogeneous catalysis, first principle, oxidation.

1. Introduction

Since early experimental findings that oxide supported small Au nanoparticles (NPs) catalyze CO oxidation even at or below room temperature,¹⁻²⁾ many efforts have been devoted to understand the chemical factors that bring the exceptional catalytic properties of Au catalysts. However, given the complexity of supported Au NPs, details of the chemical state of the reactive species are still vague. The factors that may make supported Au NPs catalytically active have been considered thus far with the size effect,³⁻¹²⁾ electronic interaction between supporting materials and NPs,^{7,13-19)} and the presence of NP-support interface.^{6,9,18,20-26)}

A group of recent reports have attributed the origin of the excellent catalytic activity of supported Au NPs to the fact that they have smaller dimensions than previously anticipated.²⁷⁻³⁰⁾ Hutchings and co-workers found that very small Au NPs consisting of around 10 atoms each are responsible for the CO oxidation reactivity of iron-oxide-supported Au NPs.²⁷⁾ Based on experimental and theoretical studies, Lee et al. showed that oxide-

supported tiny Au6-10 NPs (consisting of 6 to 10 atoms) are active for selective propene epoxidation.²⁹⁾ Turner et al. experimentally demonstrated that supported small Au NPs (~1.4 nm) derived from Au55 NP can activate molecular oxygen, leading to moderate activity for selective oxidation of styrene.³⁰⁾ They also indicated that Au NPs with diameters of ~2 nm and above are completely inactive.³⁰⁾ Moreover, single atom reaction centers or sub-nanometer sized Au NPs are getting more attentions as a reaction centers for reactions catalyzed by supported Au NPs.³¹⁻³²⁾

Given the fact that very small Au NPs are potentially, catalytically active, the importance of low-coordinated surface atoms is gaining increasing credibility. Liu et al. found that a low-coordinated step on the Au (111) surface is reactive for CO oxidation.²⁰⁾ Moreover, comparing CO oxidation activity of the Au closed-packed surface and that of the Au12 NP, Nørskov and co-workers confirmed that a low-coordinated corner of the Au12 NP facilitates the reaction.⁵⁾ However, in a natural extension of Nørskov's findings, Illas and co-workers studied adsorption and dissociation energies of O₂ on Au25, Au38,

[†]Corresponding author

E-Mail : kimhy@cnu.ac.kr (H. Y. Kim, Chungnam Nat'l Univ.)

© Materials Research Society of Korea, All rights reserved.

This is an Open-Access article distributed under the terms of the Creative Commons Attribution Non-Commercial License (<http://creativecommons.org/licenses/by-nc/3.0>) which permits unrestricted non-commercial use, distribution, and reproduction in any medium, provided the original work is properly cited.

Au55, and Au79 NPs and found that the O₂ adsorption energy is not a simple function of coordination number or particle size.¹⁰⁾ We also found that the activity of a specific reaction center of small unsupported Au NPs for CO oxidation is not just a simple function of the Au-Au coordination number.³³⁾

Other noticeable recent studies have focused on the direct or indirect participation of the Au-support interface for catalytic oxidation.^{23-25,34-35)} These studies suggest an essential role of the Au-oxide interface for O₂ binding or oxygen supply for subsequent oxidation of CO bind to Au NP.

However, because heterogeneous catalyst is a composite material itself and we are observing the averaged external properties of comprising materials, even though the interfacial areas or the low-coordinated sites could attribute to the relatively larger portion of the total activity, their combination or synergistic effect should be always considered to understand the origin of the catalytic properties of Au-oxide catalyst systems.

In this aspect, we performed a set of density functional theory (DFT) calculations to provide insights into the origins of catalytic activity of Au NPs. We initially intend to quantitatively study the effects of the size, shape, and coordination number of Au NPs on their O₂ affinity, which is a critical step for oxidation reactions catalyzed by metal NPs, especially we discuss the O₂ affinity of our studied Au NPs considering the mechanism of catalytic CO oxidation. To focus on such intrinsic factors of Au NPs, we excluded the oxide supports. In this study, we examined the oxygen adsorption on 9 types of small unsupported Au NPs of around 1 nm in size.

2. Computational Details

In accordance with the magic number of atomic construction of small NPs, we prepared the following 6 unsupported Au NPs: Au₁₃-Icosahedrol (Ih), Au₁₃-Cubo-Octahedron (COh), Au₁₉-Octahedron (Oh), Au₃₈-Truncated-Octahedron (TOh), Au₅₅-Ih, and Au₅₅-COh (see Fig. 1). We excluded Au NPs larger than Au₅₅ because the oxygen chemistry of Au₇₉-TOh converges to that of bulk Au surface.¹⁰⁾ Experimental and theoretical studies have shown that a planar-to-non-planar turnover occurs in Au NPs with 8 atoms³⁶⁾ or 12 to 14 atoms.³⁷⁾ The exact point for this turnover is still in debate. In order to ensure the consistency in morphology over the studied Au NPs, we studied Au NPs larger than Au₁₃, the minimum Au NP size for which they clearly show 3-dimensional crystalline structure. We additionally considered two experimentally reported small Au NPs, Au₁₉-Truncated-Tetrahedron (TTet) and Au₂₀-Tetrahedron (Tet),³⁸⁻³⁹⁾ as well as a specifically designed Au₂₅ that comprises one-half

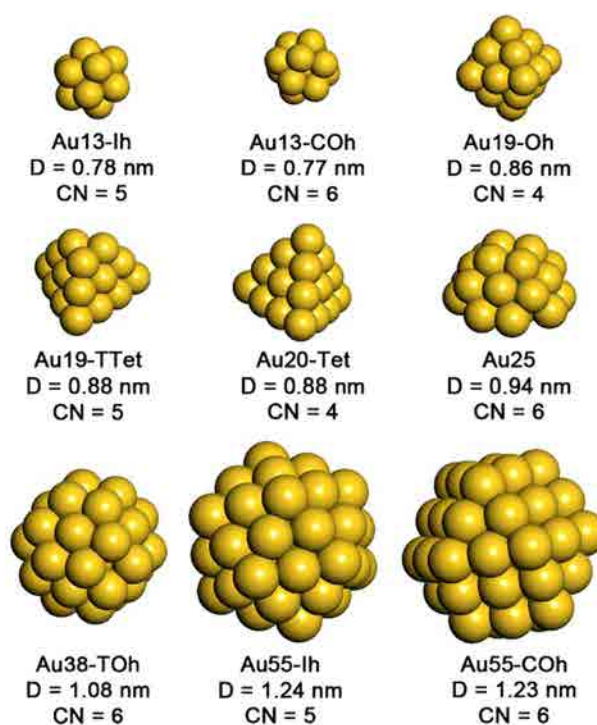


Fig. 1. Morphology and structural information of studied 9 Au nanoparticles. D and CN denote the diameter and the lowest coordination number of NPs.

of Au₃₈-TOh and is regarded as a representative of supported Au NPs.^{10,40)}

We performed GGA-level spin-polarized DFT calculations with DMol³ code.⁴¹⁻⁴²⁾ The exchange-correlation energy was functionalized with the PW91,⁴³⁾ PBE,⁴⁴⁾ and RPBE⁴⁵⁾ functionals. Roldán et al. showed that energy of adsorption of O₂ on gas-phase Au NPs is highly dependent on the exchange-correlation functional.⁴⁰⁾ They compared the performances of three general GGA-level exchange-correlation functionals, PW91, PBE, and RPBE. The PW91 functional overestimated the oxygen adsorption, whereas PBE and RPBE functionals predict rather weak oxygen-Au NP interaction.⁴⁰⁾ Generally, the oxygen binding energy calculated with the PW91 functional is rather closer to the LDA values and the RPBE functional relatively accurately describes the surface chemistry of transition metals.^{40,45-46)} The Kohn-Sham equation was expanded in a double-numeric quality basis set with polarization functions (DNP). The orbital cutoff range was 5.0 Å. The DFT semi-core pseudo potential⁴⁷⁾ was used to treat the core electrons of Au atoms. We also used a Fermi smearing method with a window size of 0.007 hartree (1 hartree = 27.2114 eV). The energy, force, and displacement convergence criteria were set to 10⁻⁵ hartree, 0.002 hartree/Å, and 0.005 Å, respectively.

Prior to evaluating O₂ and CO adsorption on Au NPs,

their structure was fully optimized. Fig. 1 shows the morphology and structural information of the studied Au NPs. The diameters of the Au NPs, calculated using the particle volumes, lie between 0.77 nm (Au13-Ih) and 1.24 nm (Au55-Ih). The coordination numbers of the most under-coordinated surface atoms of the NPs vary between 4 and 6.

To date, depending on the type of reaction intermediate, an association mechanism (O-O-CO, four-center intermediate)^{5,20,48} and a carbonate mediating mechanism (OCOO, carbonate-like intermediate)⁴⁹⁻⁵¹ have been proposed as a reaction mechanism of CO oxidation catalyzed by small NPs. However, in both cases, moderate O₂ adsorption is a minimum requirement for CO oxidation catalyzed by small metal NPs.⁴⁹ For sound operation of CO oxidation, the energy of O₂ adsorption should be sufficiently strong to prevent the thermal desorption of the O₂ molecule. Since O₂ adsorption is an initial step for CO oxidation by metal NPs irrespective of the kind of reaction mechanism,^{5,48-49} we postulate that stronger O₂ adsorption than its gas phase free energy (−0.63 eV at 298 K and 1 atm) would maximize the population of adsorbed O₂ molecules that participate in further reaction processes leading to the maximum activity. However, excessively strong O₂ adsorption is not favorable, as it may lead to unwanted permanent oxidation of NPs.

Because the under-coordinated surface atoms where the excess electrons are localized are the potential candidates for O₂ adsorption, we first examined O₂ adsorption on the edges and vertices of Au NPs.

3. Results and Discussion

Fig. 2 and Table 1 show the strongest O₂ adsorption geometry and corresponding energy of adsorption of studied NPs. Trends in O₂ adsorption energy in Table 2 substantially shows that the PW91 predicts the strongest O₂ adsorption whereas the RPBE predicts the weakest O₂ adsorption energy. We found, however, that the O₂ adsorption geometry is not dependent to the choice of the GGA-functionals. Irrespective of the GGA-functionals, the O-O bond distance of the adsorbed O₂ molecule was substantially elongated relative to that of the gas phase O₂ molecule (1.24 Å) being the clear evidence of the electron flow from the Au NP to the adsorbed O₂ mole-

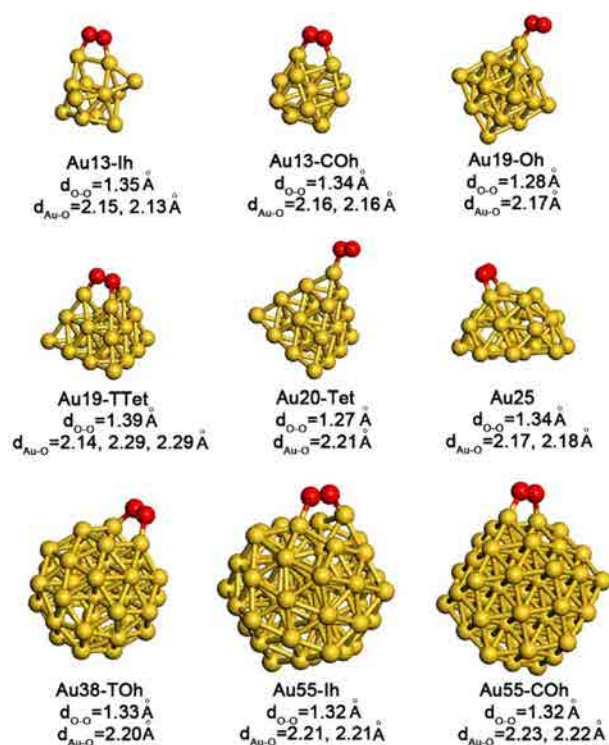


Fig. 2. Most favorable O₂ adsorption geometry of studied Au NPs. $d_{\text{O-O}}$ and $d_{\text{Au-O}}$ denotes O-O bond length of the adsorbed O₂ molecule and Au-O distance.

Table 2. Energy of sequential adsorption of CO and O₂ of selected Au nanoparticles.

	Au38-TOh	Au55-Ih	Au55-COh
ΔE_{CO} (eV)	−0.76	−0.85	−0.82
$\Delta E_{\text{CO}}^{\text{O}_2}$ (eV)	−0.31	−0.11	−0.02

cule and the presence of the chemical interaction between them. Even the RPBE functional is the most recent and relatively accurately describes the oxygen chemistry of transition metal surfaces. Table 1 shows that the RPBE functional mostly produces positive O₂ adsorption energy on Au NPs larger than the Au13. As the elongated O-O bond distance is the evidence of the chemical interaction between the O₂ molecule and the Au NP (see Fig. 2), we chose the PBE functional that produces weak but negative O₂ adsorption over studied Au NPs for further discussion.

As we anticipated, the most favorable O₂ adsorption

Table 1. Energy of O₂ adsorption of studied Au nanoparticles.

ΔE_{O_2} (eV)	Au13 Ih	Au13 COh	Au19 Oh	Au19 TTet	Au20 Tet	Au25	Au38 TOh	Au55 Ih	Au55 COh
RPBE	−1.73	−0.13	0.06	0.04	0.24	0.14	−0.01	0.06	0.27
PBE	−1.96	−0.36	−0.17	−0.14	0.04	−0.17	−0.21	−0.14	−0.03
PW91	−2.04	−0.40	−0.22	−0.18	0.03	−0.20	−0.37	−0.22	−0.07

occurs at the corners and vertices of NPs (see Fig. 2). Among the 9 studied Au NPs, the Au13-Ih ($\Delta E_{\text{O}_2} = -1.96$ eV), for which the O₂ adsorption causes a severe structural change, interacts most strongly with an O₂ molecule (see Fig. 3), whereas the other studied Au NPs weakly bind an O₂ molecule. We believe that the low O₂ binding energies of other Au NPs for example Au19-TTet and Au55-Ih are accompanied by the extremely short life span of the adsorbed O₂ molecule. Therefore, further CO oxidation reaction would not occur or CO₂ production would be very low. We postulate that our unsupported Au NPs, except for the Au13-Ih, are by themselves not good catalysts for CO oxidation.

However, it should be noted that almost 80 % of O₂ adsorption energy of the Au13-Ih is attributed to the energy gained by the adsorption-driven structural change. Such structural evolution has also been observed in our previous study of CO oxidation by the Ag13-Ih.²⁸⁾ Spontaneous structural evolution is energetically plausible because the final structure of the Au13 NP generated after O₂ adsorption is more stable than the Au13-Ih, by as much as 1.60 eV (Fig. 3). An O₂ molecule draws electrons from the contacting Au atoms and leads to positively charged Au atoms. Such electron redistribution causes an electrostatic repulsion between the positively charged Au atoms, resulting in a structural evolution of the Au13-Ih NP. However, if we exclude the energy gained by the structural change of the Au13-Ih, the energy of O₂ adsorption is decreased to -0.36 eV (Fig. 3). This confirms that the strong O₂ adsorption of the Au13-Ih is mostly due to the adsorption-driven structural change.

We introduced the Au13-Ih and the Au13-COh in order to ensure the consistency in morphology over the studied Au NPs. However, these are not the ground state structure of the Au13 NP. The disordered form of the Au13-Ih which is shown in Fig. 3 is energetically more stable as much as -1.60 eV than the Au13-Ih and -0.97 eV than the Au13-COh. Oviedo and Palmer reported that there are many structural isomers of Au13 NPs and pointed out that the disordered Au13 is energetically more stable than crystalline ones.⁵²⁾ Our present results also confirm that the disordered form of the Au13 NPs is energetically more stable than crystalline Au13 NPs. Noticeably, Oviedo and Palmer showed that the energy gaps between the structural isomers of the Au13 NP are very narrow.⁵²⁾ Therefore, even though we used the Au13-Ih as an initial structure, spontaneous structural transformations between the isomers would be observable even at room temperature. We believe that the structural fluxionality of the Au13 NP would contribute to the catalytic activity.

The fact that the structural fluxionality of very small NPs may advantageous to O₂ adsorption was proposed by Lopez and Nørskov on unsupported Au10 NP,⁵³⁾ Yoon et

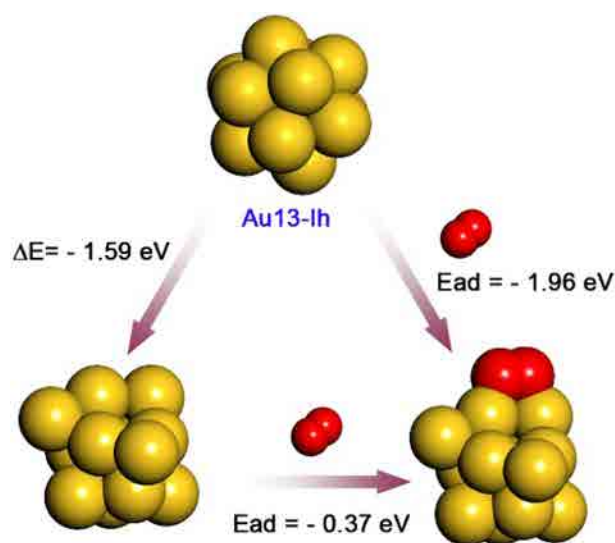


Fig. 3. O₂ adsorption on the Au13-Ih. The adsorption-driven structural change occurs during O₂ adsorption; more than 80 % of total adsorption energy is attributed to the energy gained by the structural change of the Au13-Ih.

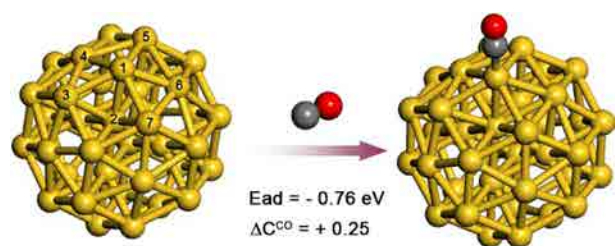


Fig. 4. Electron donation by CO adsorption. A CO molecule donates 0.25 excess electrons to the Au38-TOh (ΔC^{CO}). Most of the excess electrons are distributed to seven numbered Au atoms. Of these, two Au atoms, Au1 and Au2, draw about 46 % and 16 % of electrons, respectively. Here color codes are gold = Au, gray = carbon, and red = oxygen.

al. on MgO supported Au8 NP,¹⁹⁾ Remediakis et al. on rutile TiO₂ supported Au10 NP.²²⁾ Considering our results on the Au13-Ih and reported ones on CO oxidation by small Au NPs,^{19,22,53)} such adsorption-driven structural change generally occurs on very small Au NPs irrespective of the presence of supporting oxides.

Our results show that although the coordination number, size, or morphology of crystalline unsupported Au NPs affects on their O₂ adsorption chemistry, there is no clear quantitative relationship between the energy of O₂ adsorption and the coordination number, size, or morphology of Au NPs composed of 13 to 55 atoms (the Au13-Ih is an exception). None of these factors can dominantly control the catalytic activity of small Au NPs. In fact, the Au55-Ih and the Au19-Oh slightly strongly bind an O₂ molecule than the Au55-COh and the Au19-TTet. How-

ever, the differences in O₂ adsorption energy are not enough to make the former NPs more reactive than the later NPs.

To our best knowledge, previous studies on the relationship between the size, shape and coordination number of small Au NPs and their surface chemistry just reported that some specific Au NPs show better or worse properties than others.^{3,10,40} Information is fragmentary to deduce the general rule. In the size range of our NPs, except for the Au13-Ih, it is likely not true that the smaller NPs are always more reactive than the larger NPs and that the NPs with the lower-coordinated surface atom ensure higher reactivity.

The Au20-Tet (coordination number = 4) that very weakly or not at all binds an O₂ molecule irrespective of the GGA-functionals confirms our speculation (Table 1). Li et al. experimentally found that the Au20-Tet has extremely high HOMO-LUMO gap (1.8 eV) and suggested that such high energy gap makes the NP chemically inert.³⁸ We also found that the calculated HOMO-LUMO gap of the Au20-Tet is as high as 1.82 eV which is closely coincides with the experimental value reported by Li et al.¹⁹

Sometimes the presence of one kind of molecule affects the adsorption of a molecule of another kind,⁵⁴⁻⁵⁵ as well as negatively charged NPs could lead to strong binding of O₂ molecules.⁴⁹⁻⁵¹ Under operating conditions of CO oxidation, the catalysts are exposed to an O₂-CO mixture. A CO molecule plays a role of an electron donor, and an O₂ molecule does a role of an electron acceptor;⁴⁹ thus, co-adsorption of CO and O₂ molecules or sequential adsorption of CO and O₂ may enhance the O₂ adsorption chemistry on Au NPs. Table 2 shows adsorption energies of CO on Au38-TOh, Au55-Ih, and Au55-COh. These NPs strongly bind CO molecules. According to Mulliken charge analysis on the Au38-TOh, a CO molecule indeed donates electrons to Au NP (Fig. 4). These electrons are distributed to nearby Au atoms. Specifically, about 46 % of electrons are localized to the Au atom that directly interacts with the CO molecule (Au1 in Fig. 4), and 16 % of electrons are localized to the sub-surface Au atom (Au2 in Fig. 4). In Table 2, we also found that an electron donation from a CO molecule to unsupported Au NP is insufficient to facilitate O₂ adsorption. Variation in the energy of O₂ adsorption in the presence of a pre-existing CO molecule is marginal (see Table 2). We found that the CO-O₂ co-adsorption is not a main factor that originates the excellent CO oxidation activity of Au NPs.

We found that the exceptional catalytic activity of supported Au NPs does not mainly originate from the intrinsic nature of crystalline Au NPs larger than Au13. We think that the contributions of the following factors are presumably essential for the exceptional catalytic activity of Au NP catalysts.

(1) The NP-support electronic interaction. The Au NP is preferentially located on the defects of supporting oxides.^{18-19,22,56-57} Therefore, an electron interaction between an Au NP and the supporting material is inevitable. Moreover, in-depth studies on such electronic interaction converge to the question of how the supporting material charges Au NPs and what type of charged Au species is the reactive center for CO oxidation. The answer is, however, still unclear. We speculate that the oxygen vacancies on the supporting oxide can donate some charge to Au atoms at the NP-support interface and that these negatively charged Au atoms may enhance O₂ binding.

(2) The NP-support interface as a binding site for an O₂ molecule. Previous computational studies have already reported that such O₂ adsorption at the NP-support interface is feasible.^{19,22} The NP-support interface may contribute to O₂ adsorption by providing a new O₂ adsorption site. In this case, a metal ion of the supporting oxide or an oxygen vacancy near the NP-support interface would anchor a gas-phase O₂ molecule.

(3) Structural fluxionality of Au NPs. This is limited to very small Au NPs.^{19,22} Our Au13-Ih is a typical example of how the structural fluxionality of Au NPs affects their oxygen adsorption chemistry (Fig. 3).

Note that, for our unsupported Au NPs, the first two factors produced by the NP-support interface are completely excluded. We found that the unsupported Au NPs larger than the Au13-Ih (involving the Au13-COh) cannot bind O₂ sufficiently strongly to ensure CO oxidation activity. Therefore, if one finds that somewhat large supported Au NPs catalyze CO oxidation, the first two factors are responsible for their CO oxidation activity. The activity does not come from Au NPs themselves. On the other hand, the Au NPs that are sufficiently small for the adsorption-driven structural change to occur are good catalysts themselves, irrespective of the contributions of supporting materials. The computational finding of Remediakis et al.²² that the rutile-TiO₂-supported Au10 NP can bind O₂ molecule without participation of the NP-support interface supports our statement that such very small Au NPs can catalyze CO oxidation without the help of supporting materials.

4. Conclusion

In summary, as functions of the size, coordination number, and shape of unsupported Au NPs, we studied the oxygen adsorption chemistry of various unsupported Au NPs around 1 nm. We found that none of these factors can dominantly control the catalytic activity of small Au NPs. There is no clear quantitative relationship between the energy of O₂ adsorption and the coordination number, size, or morphology Au NPs composed of 13 to 55

atoms (the Au₁₃-Ih is an exception). We found that energetically most favorable O₂ adsorption is observed in the Au₁₃-Ih, the smallest Au NP, with the help of the structural fluxionality of such very small Au NPs. From the recent experimental studies reporting that tiny Au NPs composed of around 10 atoms are the reactive species for CO oxidation, our computational study indicates that such experimental results are originated from the structural fluxionality of tiny Au NPs. We also suggest that there is the size-threshold in Au NPs, where the smaller Au NPs can catalyze CO oxidation without the help of supporting materials whereas the support-NP interaction is required to activate larger Au NPs.

Acknowledgement

This work was supported by research fund of Chungnam National University.

References

1. M. Haruta, T. Kobayashi, H. Sano and N. Yamada, *Chem. Lett.*, **16**, 405 (1987).
2. M. Haruta, *Gold Bull.*, **37**, 27 (2004).
3. L. Barrio, P. Liu, J. A. Rodriguez, J. M. Campos-Martin and J. L. G. Fierro, *J. Chem. Phys.*, **125**, 164715 (2006).
4. M. S. Chen and D. W. Goodman, *Science*, **306**, 252 (2004).
5. H. Falsig, B. Hvolbaek, I. S. Kristensen, T. Jiang, T. Bligaard, C. H. Christensen and J. K. Norskov, *Angew. Chem. Int. Ed.*, **47**, 4835 (2008).
6. T. Fujitani, I. Nakamura, T. Akita, M. Okumura and M. Haruta, *Angew. Chem. Int. Ed.*, **48**, 9515 (2009).
7. H. Hakkinen, S. Abbet, A. Sanchez, U. Heiz and U. Landman, *Angew. Chem. Int. Ed.*, **42**, 1297 (2003).
8. B. C. Han, C. R. Miranda and G. Ceder, *Phys. Rev. B*, **77**, 075410 (2008).
9. T. Ishida, N. Kinoshita, H. Okatsu, T. Akita, T. Takei and M. Haruta, *Angew. Chem. Int. Ed.*, **47**, 9265 (2008).
10. A. Roldan, S. Gonzalez, J. M. Ricart and F. Illas, *ChemPhysChem*, **10**, 348 (2009).
11. M. Valden, X. Lai and D. W. Goodman, *Science*, **281**, 1647 (1998).
12. B. Yoon, P. Koskinen, B. Huber, O. Kostko, B. von Issendorff, H. Hakkinen, M. Moseler and U. Landman, *ChemPhysChem*, **8**, 157 (2007).
13. S. Chretien and H. Metiu, *J. Chem. Phys.*, **127**, 244708 (2007).
14. S. Chretien and H. Metiu, *J. Chem. Phys.*, **126**, 104701 (2007).
15. J. Graciani, A. Nambu, J. Evans, J. A. Rodriguez and J. F. Sanz, *J. Am. Chem. Soc.*, **130**, 12056 (2008).
16. Z. P. Liu, X. Q. Gong, J. Kohanoff, C. Sanchez and P. Hu, *Phys. Rev. Lett.*, **91**, 266102 (2003).
17. L. M. Molina and B. Hammer, *J. Chem. Phys.*, **123**, 161104 (2005).
18. J. A. Rodriguez, J. Evans, J. Graciani, J. B. Park, P. Liu, J. Hrbek and J. F. Sanz, *J. Phys. Chem. C*, **113**, 7364 (2009).
19. B. Yoon, H. Hakkinen, U. Landman, A. S. Worz, J. M. Antonietti, S. Abbet, K. Judai and U. Heiz, *Science*, **307**, 403 (2005).
20. Z. P. Liu, P. Hu and A. Alavi, *J. Am. Chem. Soc.*, **124**, 14770 (2002).
21. L. M. Molina, M. D. Rasmussen and B. Hammer, *J. Chem. Phys.*, **120**, 7673 (2004).
22. I. N. Remediakis, N. Lopez and J. K. Norskov, *Angew. Chem. Int. Ed.*, **44**, 1824 (2005).
23. H. Y. Kim, H. M. Lee and G. Henkelman, *J. Am. Chem. Soc.*, **134**, 1560 (2012).
24. H. Y. Kim and G. Henkelman, *J. Phys. Chem. Lett.*, **4**, 216 (2013).
25. H. Y. Kim and G. Henkelman, *J. Phys. Chem. Lett.*, **3**, 2194 (2012).
26. M. Cargnello, V. V. T. Doan-Nguyen, T. R. Gordon, R. E. Diaz, E. A. Stach, R. J. Gorte, P. Fornasiero and C. B. Murray, *Science*, **341**, 771 (2013).
27. A. A. Herzing, C. J. Kiely, A. F. Carley, P. Landon and G. J. Hutchings, *Science*, **321**, 1331 (2008).
28. G. Hutchings, *Nat. Chem.*, **1**, 584 (2009).
29. S. Lee, L. M. Molina, M. J. Lopez, J. A. Alonso, B. Hammer, B. Lee, S. Seifert, R. E. Winans, J. W. Elam, M. J. Pellin and S. Vajda, *Angew. Chem. Int. Ed.*, **48**, 1467 (2009).
30. M. Turner, V. B. Golovko, O. P. H. Vaughan, P. Abdulkin, A. Berenguer-Murcia, M. S. Tikhov, B. F. G. Johnson and R. M. Lambert, *Nature*, **454**, 981 (2008).
31. X.-F. Yang, A. Wang, B. Qiao, J. Li, J. Liu and T. Zhang, *Acc. Chem. Res.*, **46**, 1740 (2013).
32. J. Oliver-Meseguer, J. R. Cabrero-Antonino, I. Domínguez, A. Leyva-Pérez and A. Corma, *Science*, **338**, 1452 (2012).
33. H. An, S. Kwon, H. Ha, H. Y. Kim and H. M. Lee, *J. Phys. Chem. C*, **120**, 9292 (2016).
34. W. Song and E. J. M. Hensen, *Catal. Sci. Technol.*, **3**, 3020 (2013).
35. W. Song and E. J. M. Hensen, *ACS Catal.*, **4**, 1885 (2014).
36. R. M. Olson, S. Varganov, M. S. Gordon, H. Metiu, S. Chretien, P. Piecuch, K. Kowalski, S. A. Kucharski and M. Musial, *J. Am. Chem. Soc.*, **127**, 1049 (2005).
37. X. P. Xing, B. Yoon, U. Landman and J. H. Parks, *Phys. Rev. B*, **74**, 165423 (2006).
38. J. Li, X. Li, H.-J. Zhai and L.-S. Wang, *Science*, **299**, 864 (2003).
39. P. Gruene, D. M. Rayner, B. Redlich, A. F. G. van der Meer, J. T. Lyon, G. Meijer and A. Fielicke, *Science*, **321**, 674 (2008).
40. A. Roldan, J. M. Ricart and F. Illas, *Theor. Chem. Acc.*, **123**, 119 (2009).
41. B. Delley, *J. Chem. Phys.*, **113**, 7756 (2000).

42. B. Delley, *Comput. Mater. Sci.*, **17**, 122 (2000).
43. J. P. Perdew and Y. Wang, *Phys. Rev. B: Condens. Matter.*, **45**, 13244 (1992).
44. J. P. Perdew, K. Burke and M. Ernzerhof, *Phys. Rev. Lett.*, **77**, 3865 (1996).
45. B. Hammer, L. B. Hansen and J. K. Norskov, *Phys. Rev. B: Condens. Matter.*, **59**, 7413 (1999).
46. B. Hammer and J. K. Norskov, *Adv. Catal.*, **45**, 71 (2000).
47. B. Delley, *Phys. Rev. B: Condens. Matter.*, **66**, 155125 (2002).
48. H. Y. Kim, D. H. Kim, J. H. Ryu and H. M. Lee, *J. Phys. Chem. C*, **113**, 15559 (2009).
49. H. Y. Kim, S. S. Han, J. H. Ryu and H. M. Lee, *J. Phys. Chem. C*, **114**, 3156 (2010).
50. H. Hakkinen and U. Landman, *J. Am. Chem. Soc.*, **123**, 9704 (2001).
51. J. Hagen, L. D. Socaciu, M. Elijazyfer, U. Heiz, T. M. Bernhardt and L. Woste, *Phys. Chem. Chem. Phys.*, **4**, 1707 (2002).
52. J. Oviedo and R. E. Palmer, *J. Chem. Phys.*, **117**, 9548 (2002).
53. N. Lopez and J. K. Norskov, *J. Am. Chem. Soc.*, **124**, 11262 (2002).
54. W. T. Wallace and R. L. Whetten, *J. Am. Chem. Soc.*, **124**, 7499 (2002).
55. S. Chretien and H. Metiu, *J. Chem. Phys.*, **128**, 044714 (2008).
56. M. Baron, O. Bondarchuk, D. Stacchiola, S. Shaikhutdinov and H.-J. Freund, *J. Phys. Chem. C*, **113**, 6042 (2009).
57. T. Risse, S. Shaikhutdinov, N. Nilius, M. Sterrer and H.-J. Freund, *Acc. Chem. Res.*, **41**, 949 (2008).